The splicing factor Sf3b1 regulates erythroid maturation and proliferation via TGFβ signaling in zebrafish

Adriana De La Garza,[1,2] Rosannah C. Cameron,[1,2] Varun Gupta,[3] Ellen Fraint,[4] Sara Nik,[1,2] and Teresa V. Bowman[1,2,5]

[1]Department of Developmental and Molecular Biology, [2]Gottesman Institute of Stem Cell Biology and Regenerative Medicine, [3]Department of Cell Biology, and [4]Department of Pediatrics, Montefiore Hospital, Bronx, NY; and [5]Department of Medicine (Oncology), Albert Einstein College of Medicine, Bronx, NY

Key Points

- In vivo deficiency of *sf3b1* leads to defects in erythroid maturation and proliferation.

- TGFβ inhibition releases cell-cycle arrest in *sf3b1*-mutant erythrocytes, but worsens anemia.

The spliceosomal component Splicing Factor 3B, subunit 1 (SF3B1) is one of the most prevalently mutated factors in the bone marrow failure disorder myelodysplastic syndrome. There is a strong clinical correlation between SF3B1 mutations and erythroid defects, such as refractory anemia with ringed sideroblasts, but the role of SF3B1 in normal erythroid development is largely unknown. Loss-of-function zebrafish mutants for *sf3b1* develop a macrocytic anemia. Here, we explore the underlying mechanism for anemia associated with *sf3b1* deficiency in vivo. We found that *sf3b1* mutant erythroid progenitors display a G0/G1 cell-cycle arrest with mutant erythrocytes showing signs of immaturity. RNA-sequencing analysis of *sf3b1* mutant erythroid progenitors revealed normal expression of red blood cell regulators such as *gata1*, *globin* genes, and heme biosynthetic factors, but upregulation of genes in the transforming growth factor β (TGFβ) pathway. As TGFβ signaling is a known inducer of quiescence, the data suggest that activation of the pathway could trigger *sf3b1* deficiency–induced anemia via cell-cycle arrest. Indeed, we found that inhibition of TGFβ signaling released the G0/G1 block in erythroid progenitors. Surprisingly, removal of this checkpoint enhanced rather than suppressed the anemia, indicating that the TGFβ-mediated cell-cycle arrest is protective for *sf3b1*-mutant erythrocytes. Together, these data suggest that macrocytic anemia arising from Sf3b1 deficiency is likely due to pleiotropic and distinct effects on cell-cycle progression and maturation.

Introduction

The spliceosome is a macromolecular machine with the primary function of removing noncoding introns from pre–messenger RNA (mRNA). Alternative splicing that generates different isoforms of mature mRNA can greatly increase proteome diversity. Systematic RNA sequencing of human erythrocytes from progenitor stages throughout differentiation revealed complex alternative splicing at each step of erythroid maturation.[1] This finding suggests that splicing is critical for erythropoiesis, but how splicing factors impact erythroid proliferation and maturation in vivo is largely unknown.

Factors involved with pre-mRNA processing are commonly mutated in human hematopoietic diseases, especially those resulting in anemia and erythropoietic dysplasia.[2-4] For example, Splicing Factor 3B, subunit 1 (SF3B1), a core component of the spliceosome, is one of the most prevalently mutated factors in myelodysplastic syndromes (MDS).[2-4] Mutations in *SF3B1* correlate strongly with a subcategory of MDSs characterized by refractory anemia with ring sideroblasts,[5-7] although the exact mechanism that connects genotype to phenotype has not been found. Additionally, *SF3B1* itself undergoes extensive alternative splicing during erythroid differentiation, suggesting that SF3B1 could have discrete roles in distinct stages of erythropoiesis.[8]

The full-text version of this article contains a data supplement.

Uncovering the in vivo function of SF3B1 in erythropoiesis has been hampered due to the early lethality of *Sf3b1*-null mice before the formation of the blood system.[9] In contrast, zebrafish loss-of-function zygotic mutants are viable until ~3 days postfertilization (dpf) due to maternally contributed Sf3b1 protein and mRNA.[10] This maternal contribution means loss-of-function *sf3b1* mutants are functionally similar to a hypomorph, and survive to a developmental time point that allows for characterization of primitive erythroid differentiation. Previously, we demonstrated that zebrafish loss-of-function *sf3b1* mutants display a macrocytic anemia characterized by diminished hemoglobinized erythrocytes that have immature and dysplastic morphology.[10] Here, we show that the anemia caused by *sf3b1* deficiency is due to both maturation defects and a decrease in erythrocyte number. Using RNA sequencing, we identified elevated expression of transforming growth factor β (TGFβ) and p53 pathways and a decrease in the expression of cell-cycle programs in *sf3b1*-mutant *gata1:eGFP*+ erythroid progenitors. There were also extensive alterations in splicing with exon-skipping events most prevalent. Through pharmacological and genetic inhibition, we found that TGFβ signaling, but not p53, induced a cell-cycle arrest that protected *sf3b1* mutants from a more severe anemia. Our data imply that Sf3b1 regulation of erythropoiesis has pleiotropic and distinct effects on cell-cycle progression and maturation.

Methods

Zebrafish

Zebrafish were maintained as described.[11] All fish were maintained according to institutional animal care and use committee–approved protocols in accordance with Albert Einstein College of Medicine research guidelines.

Zebrafish lines

The *sf3b1*-mutant line *hi3394a* contains a viral insertion between the first and second exons of the *sf3b1* gene, resulting in a premature stop codon in exon 2.[12,13] Wild-type and heterozygous embryos are phenotypically indistinguishable from one another, thus, for all of the experiments presented in this manuscript, wild-type and *sf3b1*-heterozygous embryos are cumulatively referred to as siblings. As *sf3b1*-homozygous mutants are developmentally delayed and show defects in melanocyte development,[14] mutant embryos were age-matched for all analyses according to morphological features as best as possible. Mutant embryos die between 2 and 3 dpf, precluding analysis of later stages.[13] For flow cytometry analysis, we generated *sf3b1*[hi3394a/+];Tg(*gata1:eGFP*)[15] animals. For studies examining Tp53, we crossed *sf3b1* heterozygous to the well-established *tp53*[zdf1] mutant that has diminished Tp53 activity.[16]

Whole-mount in situ hybridization and *o*-dianisidine staining

In situ hybridization for *hbbe3*,[17] *cmyb*,[18] and *gata1*[19] was performed as described previously by Thisse et al[20] with minor modifications: before proteinase K (Roche) permeabilization, embryos were bleached after rehydration to remove pigmentation. The bleaching was done for 5 to 10 minutes using a bleaching solution of 0.8% KOH, 0.9% H_2O_2, and 0.1% Tween 20.

O-dianisidine staining was performed as described previously.[21] Briefly, dechorionated live embryos were soaked in *o*-dianisidine staining solution (0.62 mg/mL *o*-dianisidine [Sigma-Aldrich], 10.9 μM sodium acetate, and 0.65% H_2O_2) for 10 minutes in the dark, then rinsed in phosphate-buffered solution plus 0.1% Tween 20 (PBT) twice and observed under the microscope. Afterward, embryos were preserved in a 4% paraformaldehyde (PFA) solution.

For in situ hybridization following *o*-dianisidine staining, we performed the *o*-dianisidine protocol as described in the previous paragraph until the PBT rinse step; afterward, we followed the in situ hybridization steps as described previously by Thisse et al[20] with minor modifications: embryos were transferred to methanol for dehydration directly after *o*-dianisidine staining without fixing in 4% PFA. Methanol dehydration was done for 2 hours at −20°C.

Flow cytometry

For generation of single-cell suspensions, embryos were first removed from their chorions using pronase (Roche), and then homogenized by manual dissociation using a sterile razor blade followed by digestion with Liberase (Roche). For the digestion, dissociated embryos were resuspended in 1× Dulbecco phosphate-buffered saline (PBS; D-PBS) (Life Technologies) supplemented with a 1/65 dilution of 5 mg/mL Liberase and then incubated at 37°C for 6 minutes. The reaction was stopped with 5% fetal bovine serum (FBS) (Life Technologies). The cells were then filtered once through a 40-μm cell strainer (Falcon) and pelleted by centrifugation at 900*g* for 5 minutes. Cell pellets were resuspended in fluorescence-activated cell sorting buffer (0.9× D-PBS, 5% FBS, 1% Penn/Strep [Life Technologies]). 4′,6-Diamidino-2-phenylindole (DAPI) was added to a final concentration of 1 μg/mL to identify and exclude dead cells from the analysis. Samples were analyzed with a LSRII flow cytometer (BD Biosciences) and FlowJo version 10.0.8.

Cell-cycle analysis

For cell-cycle analysis, cells were prepared as described in the previous section, except after the first centrifugation, the cell pellets were resuspended in 1 mL of 4% PFA solution (Affymetrix) and incubated at room temperature for 15 minutes. Cells were pelleted again, supernatant was removed, cells were resuspended in D-PBS, and then stained with an anti–green fluorescent protein (GFP) antibody (Life Technologies). Afterward, cells were pelleted, supernatant was removed, and cells were resuspended in a D-PBS solution to which DAPI was added to a final concentration of 1 μg/mL. Samples were analyzed with an LSRII flow cytometer (BD Biosciences) and FlowJo version 10.0.8.

Erythroid cell RNA sequencing

Cell sorting. Embryos from an incross of *sf3b1* Tg(*gata1*:eGFP) fish were divided into siblings and mutants, and prepared for flow cytometry as described in "Flow Cytometry." For each sample, 30 000 *gata1*-eGFP+ cells from *sf3b1* mutant and siblings were sorted directly into 800 μL of Lysis buffer from the Quick-RNA MicroPrep kit (Zymo Research). Samples were immediately frozen at −80°C until ready to proceed to RNA extraction.

RNA extraction. We followed the Quick-RNA MicroPrep kit (Zymo Research) protocol, with minor modifications: step 3 was

omitted. The DNase-free DNA TURBO kit (Life Technologies) was used for DNA removal at the end of the extraction.

Library preparation. Quality and concentration of RNA and libraries was determined using the Bioanalyzer RNA Pico Chips, performed by the Albert Einstein College of Medicine Genomics Core facilities. Ribosomal RNA (rRNA) was removed with the RiboGone Mammalian kit (Clontech). Libraries were made following the protocol and using the reagents from the SMARTer Stranded RNA-Seq kit (Clontech).

Computational analysis and pathway analysis. RNA-sequencing data were generated from rRNA-depleted RNA for 5 sibling RNA samples and 5 mutant RNA samples. Analyses used the following genome release: D.rerio (GRcz10) and the GRCz10.85.gtf annotation file. Reads were trimmed using TRIM GALORE software to check for quality of 150-bp reads. These paired-end reads were mapped using STAR aligner (version 2.4.2a) to the reference genome. Differential expression analysis was done using DESeq2[22] and EdgeR[23] Bioconductor packages. To detect alternative splicing events, we used rMATS[24] (version 3.2.5). Reads were trimmed to fixed length of 100 bp and were remapped using STAR aligner before running rMATS. To calculate fragments per kilobase per million reads mapped, Cufflinks (version 2.2.1) was used. Pathway analysis was done with mSigDB.[25,26]

Treatment with SB431542

Embryos from an incross of *sf3b1*-heterozygous fish were treated with 25 μM TGFβ inhibitor SB431542 (Selleckchem) in the dark from 7 hours postfertilization (hpf) until 24 hpf for cell-cycle analysis or until 48 hpf for *o*-dianisidine staining. For the 48-hpf time point, drug was refreshed at 24 hpf. Doses tested were based on a previous study.[27] Control embryos were treated with equal volume of dimethyl sulfoxide (DMSO) as a vehicle control.

Morpholino injections

To knockdown *tp53* levels, we used a published translation-inhibiting morpholino.[28] Embryos from an *sf3b1*-heterozygous incross were injected with 8 ng of morpholino and compared with noninjected sibling controls.

Statistics

Each experiment was performed with a minimum of triplicate repeats. For pairwise comparisons, the Student *t* test (unpaired, 2-tailed) was used. Analysis of variance (ANOVA) with a Bonferroni false discovery rate (FDR) multitesting correction was performed when multiple groups were compared in an experiment. For comparison of probabilities, a Fisher's exact test was used.

Results

sf3b1 mutants have fewer, less mature erythrocytes

Anemia can arise for numerous reasons. We had previously determined that the anemia in *sf3b1* mutants was associated with defects in erythroid maturation as demonstrated by diminished levels of hemoglobinized cells with more immature morphology compared with their wild-type siblings.[10] Diminished erythrocyte number, defects in erythroblast maturation, or hemoglobinization can lead to a decrease in the amount of hemoglobinized cells. Based on the observation that *sf3b1*-mutant erythroid cells were at various stages of differentiation according to morphology,[10] we

hypothesized that mutants contained 2 separate pools of erythrocytes: immature, nonhemoglobinized cells and more mature cells that are hemoglobinized. To further explore this hypothesis, we decided to assess the maturation state of erythrocytes using a metric independent of hemoglobinization. Normally, the early embryonic globin gene *hbbe3* is nearly absent in wild-type embryos by 48 hpf.[17] Indeed, at 36 hpf, wild-type siblings already have diminished levels of *hbbe3*, with little to no expression by 48 hpf (Figure 1A; supplemental Figure 1). In *sf3b1* mutants at 36 and 48 hpf, some embryos had a large amount of *hbbe3*-expressing cells, whereas others had none (Figure 1B; supplemental Figure 1). Similarly, *o*-dianisidine staining in 48-hpf mutant embryos also followed the same pattern: in some embryos, there is a large amount of hemoglobinized erythrocytes, whereas in other embryos hemoglobinized erythrocytes are completely absent (Figure 1C-D). This gives rise to 2 possibilities:

1. There could be 2 developmentally distinct erythrocyte populations in the mutant embryos at 48 hpf: 1 population that is immature and still expressing *hbbe3* and not functionally hemoglobinized, and 1 population that matures normally and becomes hemoglobinized; or

2. There could be a single erythrocyte population in the mutant embryos that is immature but is capable of carrying oxygen by 48 hpf.

To distinguish between both possibilities, we performed sequential *o*-dianisidine staining followed by *hbbe3* in situ hybridization in the same *sf3b1*-mutant embryos (Figure 1E). Using this approach, we can visualize whether the *hbbe3*-expressing cells also possess functional hemoglobin within an individual embryo. The results showed that, in *sf3b1* mutants, all *o*-dianisidine–positive cells are also positive for *hbbe3* expression (Figure 1F). The failure of mutant erythroid cells to downregulate *hbbe3* is strong evidence that mutant red blood cells are not maturing like wild-type cells. Combined, this evidence suggests that the diminishment in hemoglobinized erythrocytes in *sf3b1* mutants at 48 hpf results from the mutants having fewer erythrocytes, which are also less mature.

Erythroid progenitors arising from both primitive and erythroid-myeloid progenitor (EMP)-derived definitive waves are present during the developmental time points analyzed in Figure 1. To determine whether there were defects in EMP-derived erythropoiesis, we performed in situ hybridization for the progenitor marker *c-myb* at 30 and 36 hpf and *gata1* at 30 hpf in siblings and *sf3b1* mutants (supplemental Figure 2A-B). Expression of both *c-myb* and *gata1* within the posterior blood island (PBI) region where EMPs form was similar between siblings and *sf3b1* mutants. Furthermore, we examined erythroid progenitor levels at 24 and 36 hpf within the PBI using Tg(*gata1:eGFP*) zebrafish,[15] in which enhanced GFP (eGFP) marks erythroid cells, and observed high levels of *gata1:eGFP* within the PBI region of mutant embryos (supplemental Figure 2C). In a prior study,[10] we examined the expression of a myeloid-associated EMP marker (*pu.1*) and also found normal expression in *sf3b1* mutants. Combined these data indicate that EMP formation is unaffected when levels of *sf3b1* are limiting. Mutants become progressively unhealthier from 48 to 72 hpf, thus we were not able to assess differentiation of EMP-derived erythrocytes. Based on these data, we conclude that the majority of the erythrocyte defects observed up to 48 hpf in *sf3b1* mutants are due to defects in primitive wave-derived cells.

Figure 1. Sf3b1 regulates erythrocyte number and maturation. (A-D) In situ hybridization of early globin *hbbe3* (A-B) and *o*-dianisidine staining (C-D) in siblings (Sib) (A,C) and *sf3b1* mutant (mut) (B,D) at 48 hpf. For mutants, example of a high signal embryo is shown on the left and an example of a mutant with low signal is shown on the right. Numbers in the lower right denote number of embryos that displayed a similar phenotype to the image. Graphs on the right denote the percentage of embryos with the designated phenotype. (E) Schematic representing the experimental flow to measure *hbbe3* levels in *o*-dianisidine–positive erythrocytes by sequential staining. *O*-dianisidine staining was performed first followed by *hbbe3* in situ hybridization in the same embryo, thus consecutively labeling oxygenated and immature erythrocytes. (F) *O*-dianisidine staining (top) followed by in situ hybridization of *hbbe3* (bottom) in the same *sf3b1*-mutant embryos at 48 hpf (2 examples shown). Inset to the right shows a higher magnification view of area boxed in the image on the left. (A-D,F) In situ stain nitroblue tetrazolium, *o*-dianisidine stain; original magnification ×6, inset ×12. Med, medium.
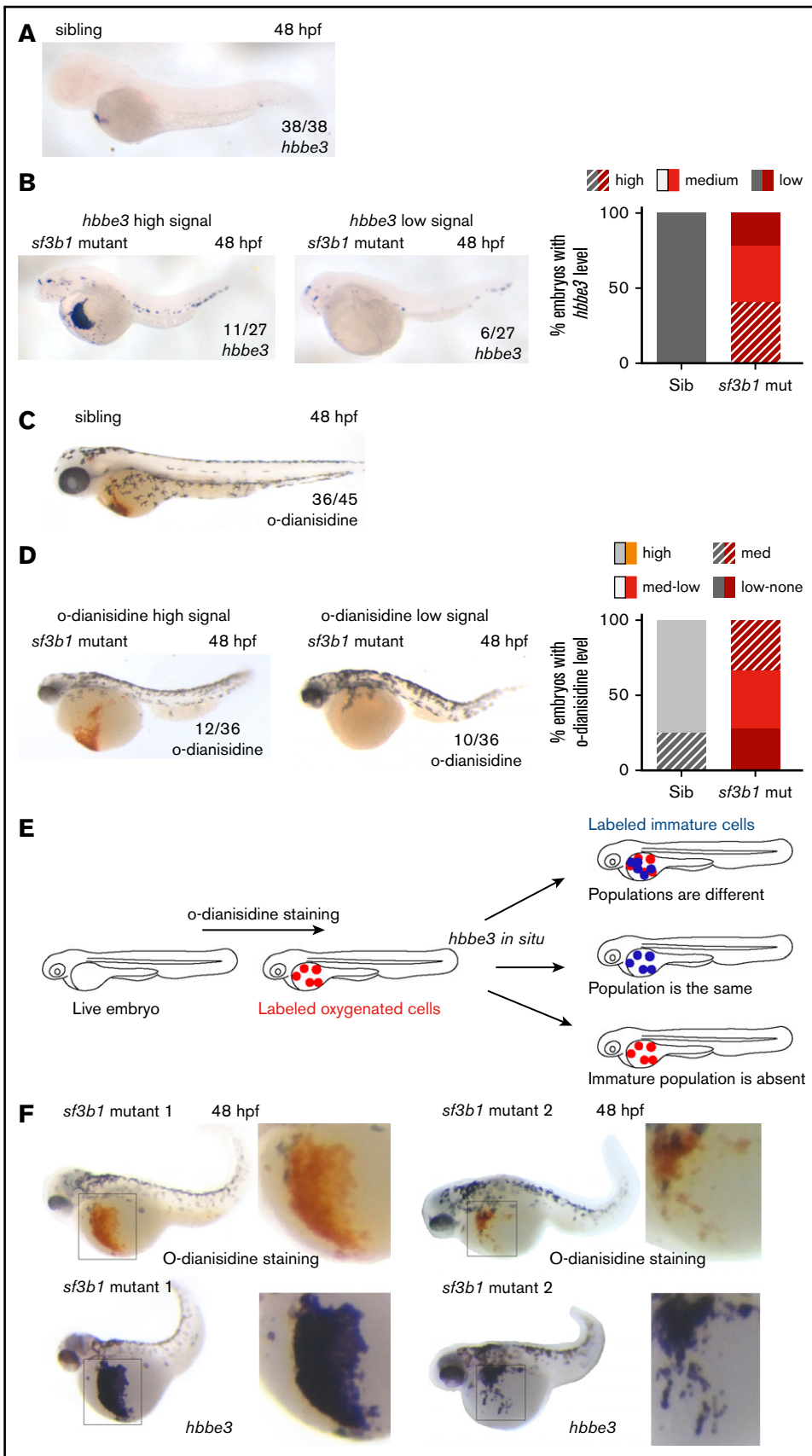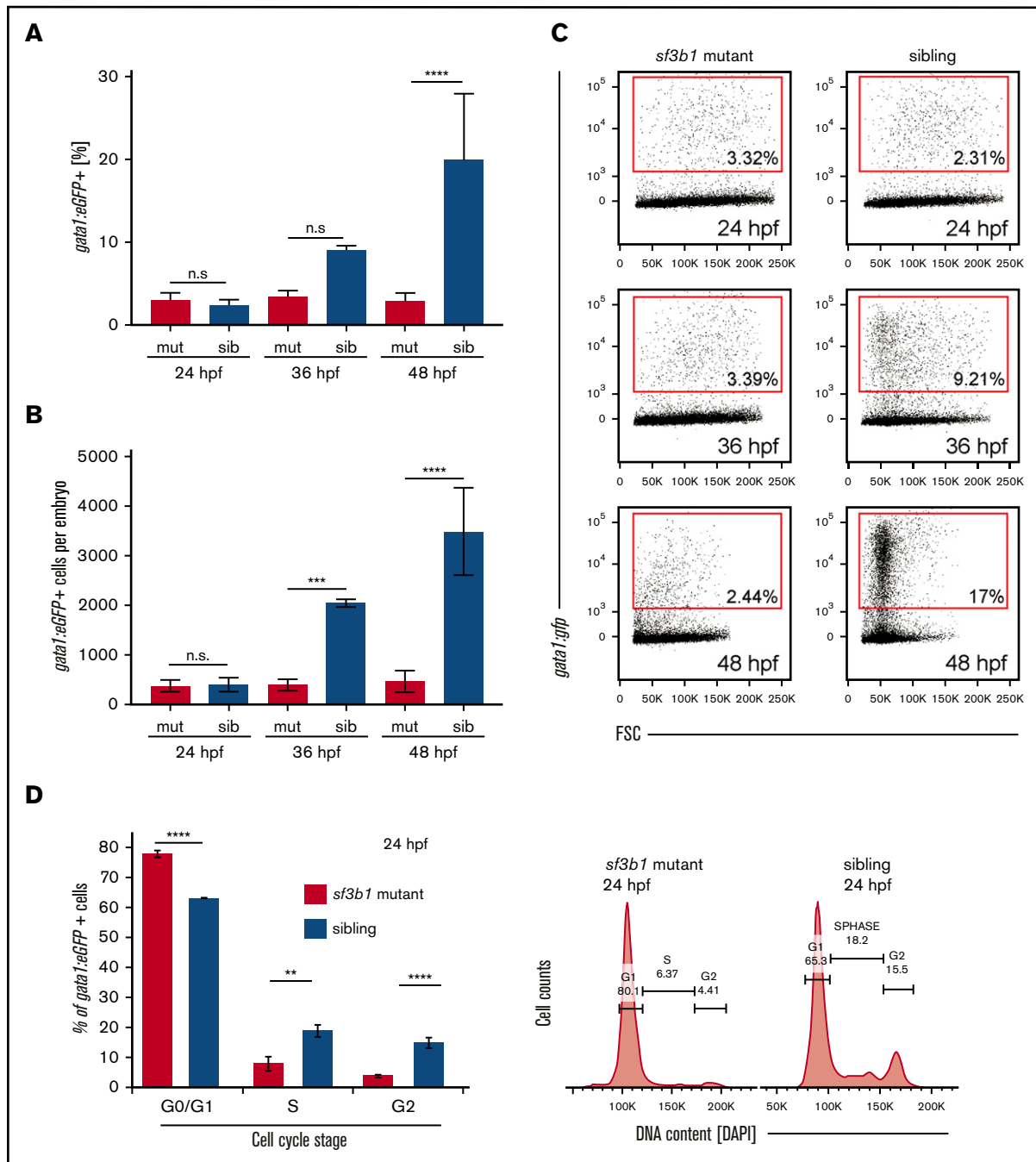
Figure 2. Loss of *sf3b1* triggers a G0/G1 cell-cycle arrest in erythroid progenitors. (A-B) Graph quantifying *gata1:eGFP*^{+} cells in *sf3b1*-mutant and wild-type siblings at 24, 36, and 48 hpf. (A) Percentage of *gata1:eGFP*^{+} cells. (B) Absolute number of *gata1:eGFP*^{+} cells per embryos. (C) Representative flow cytometry plots for panels A and B. (D) Graph quantifying the percentage of *gata1:eGFP*[+] erythrocytes in G0/G1, S, or G2/M phases of the cell cycle at 24 hpf. Representative flow cytometry histograms of erythrocyte DNA content as measured by DAPI fluorescence intensity on *sf3b1* mutants and siblings. All experiments were done in biological triplicates. Statistical significance calculated by an ANOVA with a Bonferroni FDR multitesting correction. **$P < .01$, ***$P < .001$, ****$P < .0001$. FSC, forward scatter; n.s., not significant.

Cell-cycle arrest is triggered in *sf3b1*-mutant erythrocytes

To quantify erythrocyte numbers at 24, 36, and 48 hpf, we measured the frequency and absolute number of *gata1:eGFP*^{+} cells in siblings and *sf3b1* mutants using flow cytometry (Figure 2A-C). No difference was observed between siblings and mutants

at 24 hpf. Both frequency and absolute number of *gata1:eGFP*[+] erythrocytes were diminished at 36 hpf compared with siblings with the effect even more pronounced by 48 hpf.

These findings suggest a lack of erythrocyte expansion or elevated cell death. From our previous work, we observed no increase in active Caspase-3 staining in the blood-forming regions of *sf3b1*

mutants compared with siblings, suggesting apoptosis is not driving the lower erythrocyte numbers in mutants.[10] Next, we tested whether differences in proliferation could underlie the decrease in erythrocyte frequency. Cell-cycle status of *gata1:eGFP*[+] erythroid progenitors from siblings and *sf3b1* mutants at 24 hpf was quantified via flow cytometry using DAPI fluorescence as a metric for DNA content (Figure 2D). Mutant cells had an increased amount of cells in the G0/G1 phase (2N content of DNA) and a greatly diminished amount of cells in S phase in comparison with their wild-type siblings. These results suggest that *sf3b1* loss in erythrocytes triggers a G0/G1 cell-cycle arrest.

Expression and splicing of the TGFβ and p53 pathways are altered in *sf3b1*-mutant erythrocytes

To understand the mechanism behind the erythroid defect in *sf3b1* mutants, we conducted RNA sequencing of purified erythroid progenitors from wild-type and mutant siblings at 24 hpf when differences in erythroid cell number are not yet evident in the mutant embryos. This permitted us to capture some of the earliest transcriptional changes leading to erythrocyte dysfunction. We sorted *gata1:eGFP*^{+} cells from siblings and *sf3b1* mutants at 24 hpf. Stranded RNA-sequencing libraries were then generated from rRNA-depleted RNA samples. Five independent biological replicates were analyzed. On average, ~28 million paired-end 150-bp sequencing reads were acquired per sample. DE-Seq2[22] and EdgeR[23] were used to determine differential gene expression (defined as twofold change, FDR $P < .05$) between control sibling and mutant erythrocytes. Of the nearly 32 000 genes analyzed, 913 genes were downregulated and 774 were upregulated in *sf3b1* mutants compared with sibling control erythrocytes (Figure 3A-B; supplemental Tables 1 and 2). The heatmap shows the top 500 differentially expressed genes and clustering of the 5 replicates according to genotype (Figure 3C). Among the normally expressed genes are several erythropoiesis regulators, all embryonic globins, and most of the heme-group synthesis pathway genes (Figure 3D).

To gain insight into the affected pathways, the upregulated and downregulated gene lists were analyzed with mSigDB, a platform that computes overlaps between experimentally derived gene lists and lists of genes in known pathways.[25,26] Specifically, we compared the upregulated and downregulated gene sets in *sf3b1*-mutant erythroid progenitors to the Kyoto Encyclopedia of Genes and Genomes (KEGG) collection, which contains 186 gene sets collated for biological function.[29-31] In the upregulated gene list, spliceosome was the top enriched gene set suggesting a compensatory upregulation of splicing factors due to loss of *sf3b1* (Figure 3E; supplemental Table 3). Additionally, genes involved with the stress-activated *p53*-signaling pathway, *TGFβ*-signaling pathway, and *MAPK* were also among the top enriched pathways in the upregulated gene set. Of note, activation of both the p53 and TGFβ pathways is linked with cell-cycle arrest and cellular quiescence in hematopoietic cells.[32,33] In the down-regulated list, genes associated with hematopoietic cell line-age were among the top enriched gene set, consistent with the deregulation of erythroid maturation in *sf3b1* mutants (Figure 3F; supplemental Table 4). In line with the observed cell-cycle arrest, factors involved with the cell cycle were also significantly enriched in the downregulated genes. Together, these data show that *sf3b1*-mutant erythrocytes have deregulated expression of genes involved with hematopoietic lineage, cell cycle, and signaling.

Sf3b1 is a part of the U2 small nuclear ribonucleoprotein complex important for pre-mRNA splicing, thus we also examined how *sf3b1* loss affected mRNA splicing in embryonic erythrocytes. Differential inclusion rates across 16 766 splicing events between *sf3b1* mutants and wild-type siblings were calculated using replicate Multivariate Analysis of Transcript Splicing (rMATS).[24] Splicing events with inclusion differences ≥10% and FDR ≤0.01 were considered significantly misspliced. A total of 1357 events in 1104 genes were misspliced between *sf3b1* mutants and siblings with cassette exons being the largest group (Figure 4A; supplemental Table 5). The volcano plots show splicing events with a change in the percent spliced in (Δψ) between control siblings (<0) and *sf3b1* mutants (>0) (Figure 4B). In 82% of the misspliced transcripts, only a single differential event was detected indicating a high degree of specificity for the splicing events that are most sensitive to Sf3b1 levels. Aberrant splicing can result in the inclusion of premature nonsense codons that then trigger transcript degradation via the nonsense-mediated decay pathway.[34] We compared the misspliced genes to those differentially expressed between *sf3b1* mutants and siblings and found no significant overlap suggesting the alterations in splicing are not majorly contributing to changes in overall transcript abundance in erythroid progenitors (Figure 4C).

Altered splicing can also change the function of the protein encoded by the transcript. To determine whether particular pathways were impacted in the misspliced genes, we compared the misspliced gene list to the KEGG gene sets using mSigDB. Some of the top pathways enriched in the misspliced genes were associated with cancer (pathways in cancer, MAPK signaling, and spliceosome) (Figure 4D; supplemental Table 6). Although the overlap of the misspliced genes and differentially expressed genes was moderate, similar pathways were affected, suggesting functional convergence of altered splicing and gene expression when *sf3b1* is mutated.

Sf3b1 regulation of TGFβ is essential for erythrocyte maturation and expansion

The gene-expression data suggest that activation of the TGFβ or p53 pathways could contribute to the anemia in *sf3b1* mutants. TGFβ is a versatile pathway that plays several different roles in cellular regulation.[35] TGFβ signaling is linked to erythroid differentiation and is elevated in MDS; inhibitors of TGFβ superfamily signaling are currently being tested clinically for treatment of a variety of ineffective erythropoiesis syndromes, including MDS-associated refractory anemia.[36-38] These findings combined with the observation that genes in the TGFβ-signaling pathway are upregulated in *sf3b1*-mutant erythroid progenitors led us to test the effect of inhibiting TGFβ signaling on the erythropoietic defects in *sf3b1* mutants.

To test this hypothesis, we treated embryos with the TGFβ inhibitor SB431542, previously shown to inhibit *Smad3*-dependent TGFβ signaling in zebrafish, and then determined the effects on cell-cycle progression and maturation (Figure 5A).[39] TGFβ signaling can suppress erythroid progenitor proliferation,[40] thus we determined whether the cell-cycle arrest in *sf3b1*-mutant erythrocytes was due to TGFβ signaling. Cell-cycle status of 24-hpf *sf3b1*-mutant *gata1:eGFP*[+] erythroid progenitors was assessed in embryos treated with 25 μM SB431542 or DMSO control (Figure 5A). There was a significant increase of *gata1:eGFP*^{+} cells in S phase
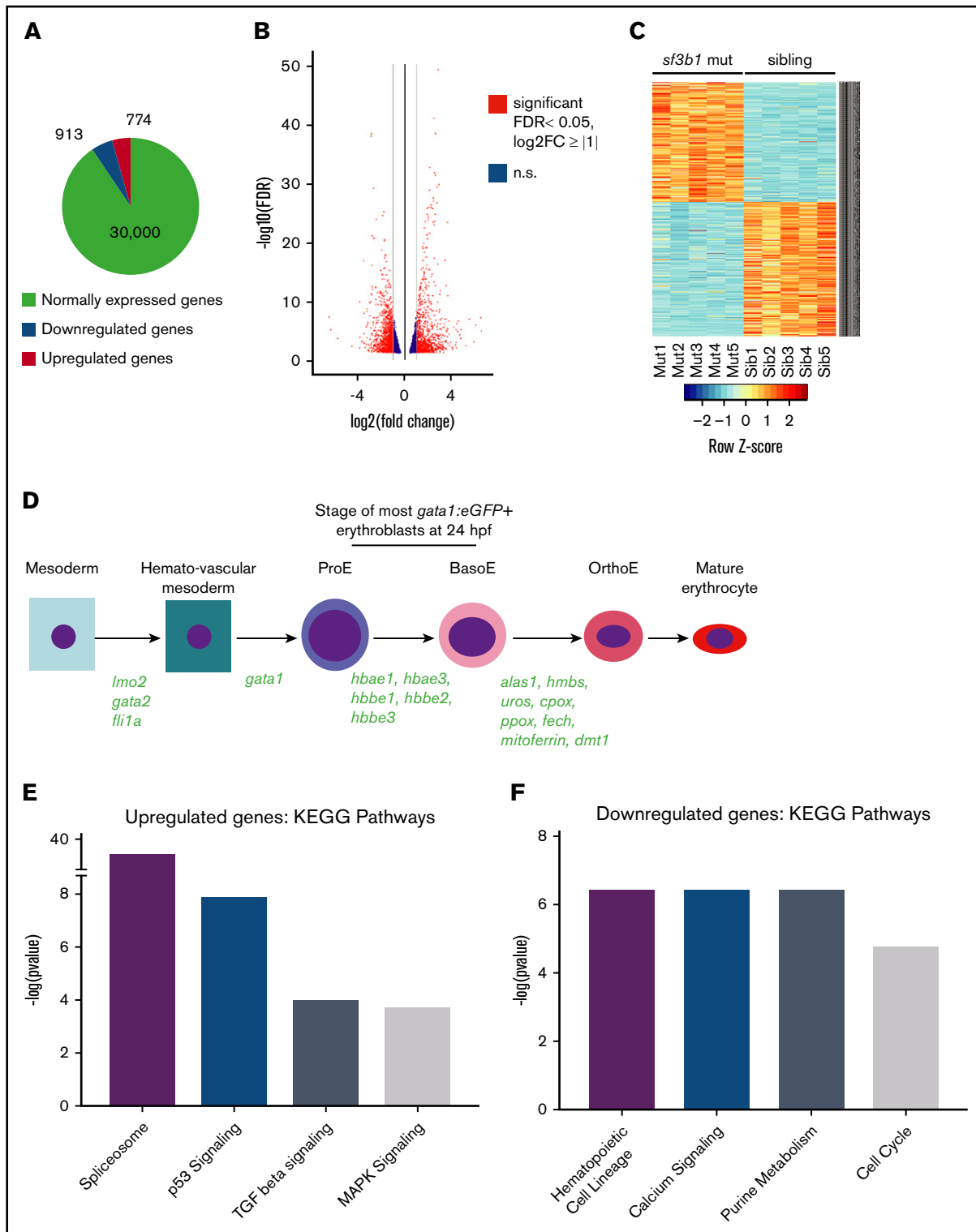
Figure 3. TGFβ- and Tp53-regulated genes are upregulated in *sf3b1*-mutant erythroid progenitors. (A) Representative chart of gene expression in *gata1:eGFP*+ cells from *sf3b1* mutants. (B) Volcano plot displaying differentially expressed genes between *gata1:eGFP*+ cells from *sf3b1* mutants and siblings. Significant differences are defined as FDR <0.05 and log2 fold change (FC) >1. Gray lines denote the fold-change threshold. (C) Heatmap of top 500 differentially expressed genes between *gata1: eGFP*+ cells from *sf3b1* mutants and siblings. Each row is a gene and each column is a replicate. Mutant samples are shown on the left and sibling samples are shown on the right. (D) Schematic highlighting normally expressed hematopoietic genes in *sf3b1*-mutant erythrocytes and the stage at which they begin to be expressed (gene names in green). (E-F) Representative charts of significantly altered KEGG pathways in genes upregulated (E) or downregulated (F) in *sf3b1*-mutant erythroid progenitors compared with sibling controls as determined by mSigDB analysis. BasoE, basophilic erythroblast; OrthoE, orthochromatophilic erythroblast; ProE, proerythroblast.
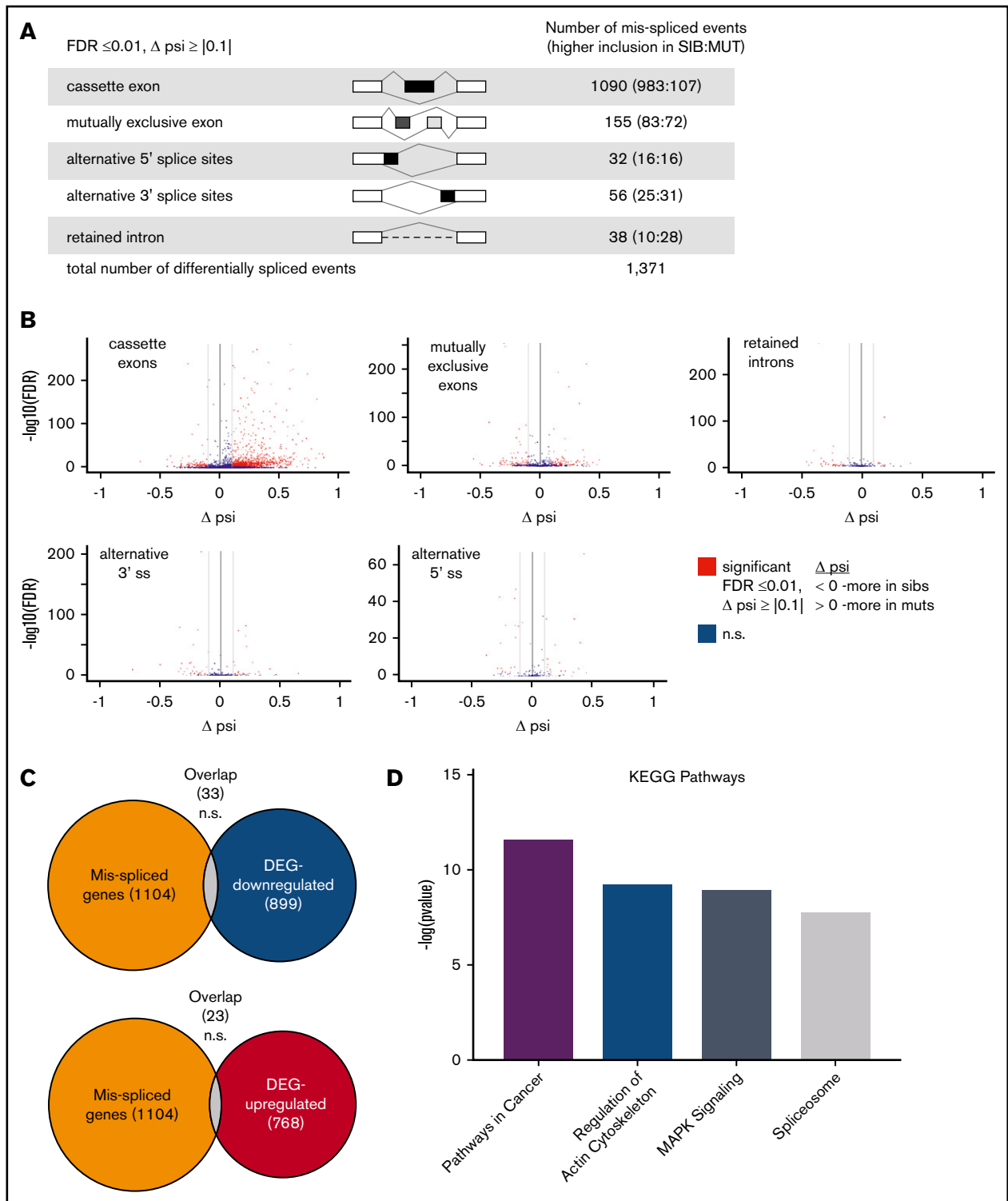
Figure 4. Cancer-associated genes are misspliced in *sf3b1*-mutant erythroid progenitors. (A) Schematic of the different splicing events detected by analysis with rMATS. The numbers in the parentheses (n1:n2) indicate the number of significant events that have higher inclusion level for sibling (n1) or for mutant (n2). (B) Volcano plot of differential splicing events between *gata1:eGFP*+ cells from *sf3b1* mutants and siblings. Significant differences are defined as FDR ≤0.01 and Δψ > |0.1|. Gray lines denote the Δψ threshold. (C) Venn diagrams showing overlap of misspliced transcripts with differentially expressed genes. Probability of overlap calculated by hypergeometric distribution. (D) Representative charts of significantly altered KEGG pathways in misspliced transcripts in *sf3b1*-mutant erythrocytes compared with sibling controls as determined by mSigDB analysis. DEG, differentially expressed genes; psi, percent spliced in; ss, splice site.
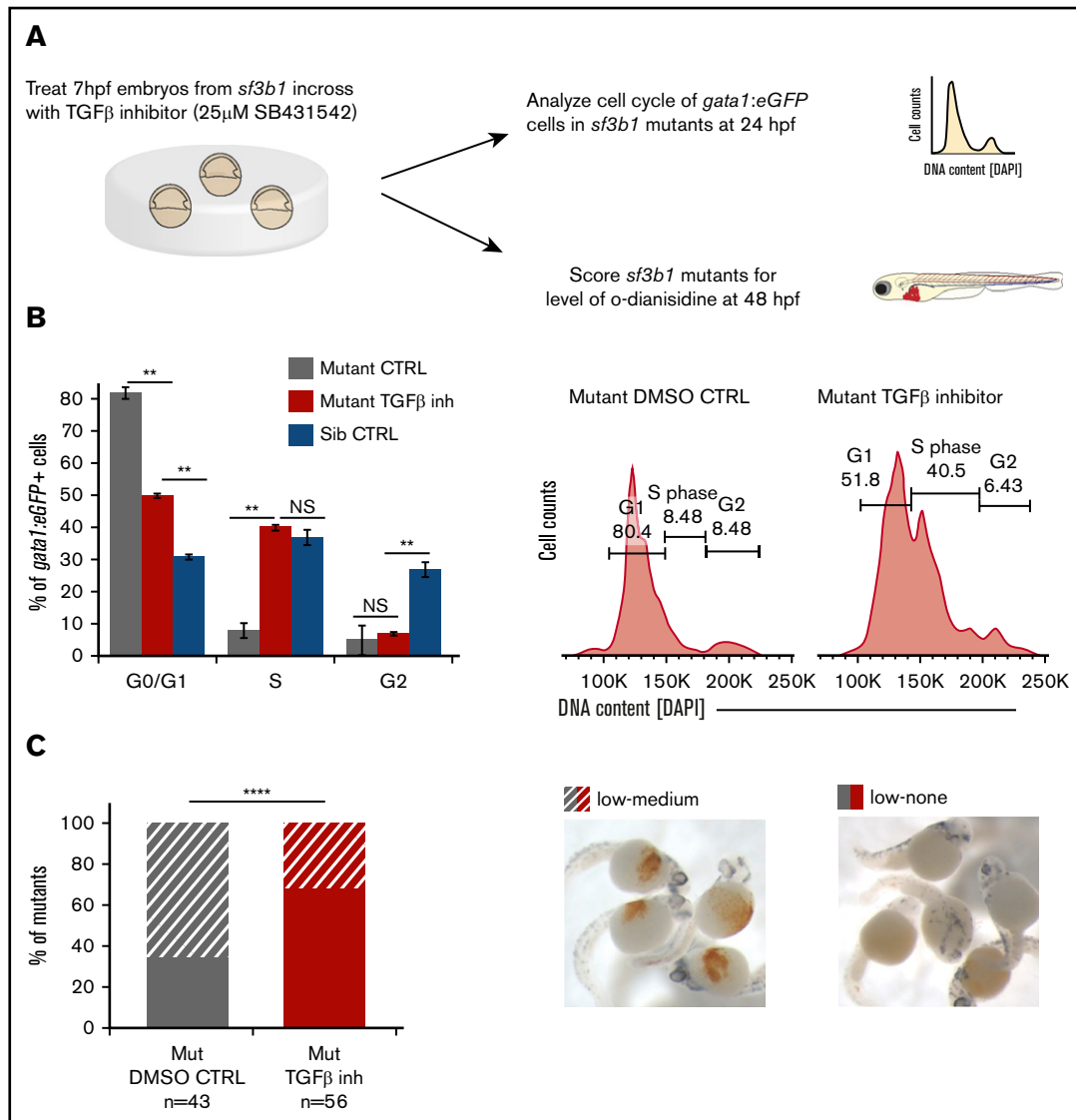
Figure 5. TGFβ-mediated cell-cycle arrest is protective for *sf3b1*-mutant erythrocytes. (A) Schematic of experiment to determine whether inhibition of TGFβ signaling alters erythroid cell-cycle arrest or anemia in *sf3b1* mutants. (B) Graph quantifying the percentage of *gata1:eGFP*+ erythrocytes in G0/G1, S, or G2/M phases of the cell cycle at 24 hpf in *sf3b1* mutants treated with a DMSO control or 25 μM of the TGFβ inhibitor SB431. Cell cycle of wild-type siblings is included for comparison. Representative flow cytometry histograms of erythrocyte DNA content as measured by DAPI fluorescence intensity on *sf3b1* mutants treated with a DMSO control or 25 μM SB431542 are shown on the right. Statistical significance calculated by an ANOVA with a Bonferroni FDR multitesting correction. (C) Graph showing frequency of *sf3b1* mutants with designated levels of o-dianisidine–positive oxygenated erythrocytes at 48 hpf after treatment with DMSO control or 25 μM SB431542. Total number of mutants analyzed per treatment group is listed below the graph. Images of *sf3b1*-mutant embryos with low-medium or low-none o-dianisidine–positive cells are shown to the right. Significance of comparison between groups determined by the Fisher's exact test. All experiments were done in biological triplicates. **P < .01, ****P < .0001. (C) O-dianisidine stain; original magnification ×4.

and concomitant decrease of cells in G0/G1 (Figure 5B). Next, we examined the impact on erythroid maturation at 48 hpf and found the surprising result that *sf3b1* mutants treated with 25 μM SB431542 displayed a more severe anemia than those treated with the DMSO control (Figure 5C). Together, these data indicate that TGFβ signaling triggers a G0/G1 cell-cycle arrest in *sf3b1*-mutant erythrocytes that protects the mutant cells from later maturation defects and/or cell death.

Dampening p53 signaling can improve anemia in some zebrafish mutants including those with mutations in ribosomal components.[28] Tp53 is a potent inducer of cell-cycle arrest, thus we examined

whether knockdown of *tp53* using a well-established morpholino[28] could further improve cell-cycle progression in *sf3b1* mutants treated with the TGFβ inhibitor (supplemental Figure 3A-B). We observed no further improvement in cell-cycle progression upon *tp53* knockdown compared with TGFβ inhibition alone. Next, we determined whether diminished Tp53 activity affects erythroid maturation by measuring o-dianisidine levels in *sf3b1;tp53*[zdf1] double mutants, which have diminished Tp53 activity.[16] The frequency of *sf3b1* mutants with medium-low o-dianisidine-positive erythrocytes was decreased in *sf3b1; tp53* double mutants compared with single mutants (supplemental Figure 3B). The same result was seen in *sf3b1* mutants injected with the *tp53* morpholino (data not shown). Double *sf3b1;tp53*

mutants treated with the TGFβ inhibitor showed the same effect as those only treated with the TGFβ inhibitor.

Discussion

This study of erythroid cell development in *sf3b1*-mutant embryos has uncovered important details about the effects of spliceosomal disruption on red blood cell biology. We found that *sf3b1* deficiency led to the production of fewer erythrocytes that show maturation defects and dysplasia.[10] Genes in the TGFβ and the p53 pathways were significantly upregulated upon *sf3b1* loss. Functionally, TGFβ pathway activity induced a G0/G1 cell-cycle arrest in *sf3b1*-mutant proerythroblasts. Pharmacological inhibition of the TGFβ pathway relieved the cell-cycle arrest, but worsened anemia. These data suggest that loss of *sf3b1* triggers a TGFβ-mediated cell-cycle checkpoint that acts to protect erythroid progenitors, possibly from aberrant differentiation due to diminished amounts of Sf3b1. Additionally, our findings suggest that TGFβ signaling plays a more prominent role in *sf3b1*-mutant anemia than Tp53. Combined, these data demonstrate a key functional difference between anemia caused by loss of *sf3b1* vs those with ribosomal defects.

Few studies have explored the function of wild-type SF3B1 in erythropoiesis. A recent report demonstrated that in vitro knockdown of *SF3B1* in human CD34$^+$ hematopoietic stem and progenitor cells results in ineffective erythropoiesis.[41] In this study, activation of the p53 pathway contributed to cell-cycle arrest and elevated apoptosis in early-stage progenitors. In zebrafish, we similarly found that the p53 pathway was activated, but, unlike in the in vitro study, this had little effect on erythropoiesis in *sf3b1*-mutant cells, indicating key functional differences in response to splicing factor deficiency in cell culture vs an animal model. There is growing evidence that the microenvironment is heavily involved in MDS and ineffective erythropoiesis.[42] Indeed, our findings in an *sf3b1*-deficient zebrafish model support a role for the microenvironment in anemia highlighting the importance of animal models in understanding how splicing factors regulate hematopoiesis.

Unlike the zebrafish *sf3b1* mutants that are homozygous loss of function, MDS-associated mutations in *SF3B1* are mainly heterozygous missense mutations.[7] The most common mutations are in the C-terminal portion of the protein most often changing lysine 700 to glutamic acid (K700E). Murine models with hematopoietic-restricted expression of *Sf3b1*$^{+/K700E}$ develop macrocytic anemia and have a G0/G1 arrest in early progenitors similar to zebrafish *sf3b1*-homozygous mutants.[43,44] The prevailing view of how MDS-associated mutations like K700E affect SF3B1 is that they change SF3B1 splice-site preferences and result in dominant neomorphic functions in splicing.[43-45] Despite these differences in splicing function, over 10% of genes misspliced in *SF3B1*-mutated MDS[46] were also misspliced in zebrafish *sf3b1*-mutant erythrocytes. At the expression level, 37% of KEGG pathways enriched in the deregulated genes in *SF3B1*-mutated MDS CD34$^+$ progenitors compared with healthy controls[47] were also enriched in the genes differentially expressed in zebrafish *sf3b1*-mutant erythrocytes. Although the zebrafish *sf3b1* loss-of-function mutants show more extensive transcriptome changes, these cellular and molecular commonalities suggest that there is some similarity between zebrafish *sf3b1* mutants and *SF3B1*-mutated MDS.

Clinically, novel TGFβ superfamily inhibitors are currently being tested for treatment of low-risk MDS, which are highly enriched for *SF3B1*-mutated MDS.[36,37] These protein-based drugs, such as sotatercept and luspatercept, work as activin ligand traps that prevent receptor-mediated activation of the pathway. These TGFβ superfamily inhibitors seem to work by inhibiting the growth differentiation factor 11 (GDF11) ligand, which results in stimulation to erythroid differentiation in late-stage erythropoiesis, distinct from the action of erythropoietin that stimulates early-stage progenitors. In zebrafish *sf3b1* mutants, treatment with TGFβ receptor kinase inhibitor SB431542 resulted in improvements in erythroid progenitor proliferation, but a worsening of anemia. Our study demonstrates that inhibition of type I TGFβ receptors have the potential to improve cell-cycle progression of arrested erythroid progenitors, but cannot improve differentiation. Future studies are warranted to examine the impact of dual treatment with both types of TGFβ inhibitors.

SF3B1-modulating drugs are also being evaluated for the treatment of patients with splicing factor-mutated MDS.[48] These drugs work via a synthetic lethal modality that leads to the selective death of splicing factor mutant cells over nonmutated cells. Our findings suggest that treatment with a TGFβ receptor inhibitor plus an SF3B1 modulator could enhance synthetic lethality to ablate splicing factor mutant clones. So far, TGFβ superfamily inhibitors show minimal long-term side effects, whereas splicing factor modulating drugs can have adverse side effects.[49] Combined treatment could result in a more robust effect at lower drug doses resulting in safer treatment.

Our study provides mechanistic insight into how Sf3b1 defects drive aberrant erythropoiesis in vivo. The findings highlight the importance of animal models to understand how defects in this highly relevant MDS-associated factor impacts erythropoiesis.

Authorship

Contribution: A.D.L.G., R.C.C., E.F., S.N., and T.V.B. performed experiments and analyzed data; V.G. performed bioinformatics analyses; and A.D.L.G. and T.V.B. wrote and edited the manuscript.

Conflict-of-interest disclosure: The authors declare no competing financial interests.

The current affiliation for A.D.L.G. is Biogen, Durham, NC.

The current affiliation for R.C.C. is Ferrier Research Institute, Victoria University of Wellington, Wellington, New Zealand.

Correspondence: Teresa V. Bowman, Albert Einstein College of Medicine, 1300 Morris Park Ave, Chanin 501, Bronx, NY 10461; e-mail: teresa.bowman@einstein.yu.edu.

References

1. Pimentel H, Parra M, Gee S, et al. A dynamic alternative splicing program regulates gene expression during terminal erythropoiesis. *Nucleic Acids Res*. 2014;42(6):4031-4042.

2. Haferlach T, Nagata Y, Grossmann V, et al. Landscape of genetic lesions in 944 patients with myelodysplastic syndromes. *Leukemia*. 2014;28(2):241-247.

3. Papaemmanuil E, Gerstung M, Malcovati L, et al; Chronic Myeloid Disorders Working Group of the International Cancer Genome Consortium. Clinical and biological implications of driver mutations in myelodysplastic syndromes. *Blood*. 2013;122(22):3616-3627, quiz 3699.

4. Yoshimi A, Abdel-Wahab O. Splicing factor mutations in MDS RARS and MDS/MPN-RS-T. *Int J Hematol*. 2017;105(6):720-731.

5. Cazzola M, Rossi M, Malcovati L; Associazione Italiana per la Ricerca sul Cancro Gruppo Italiano Malattie Mieloproliferative. Biologic and clinical significance of somatic mutations of SF3B1 in myeloid and lymphoid neoplasms. *Blood*. 2013;121(2):260-269.

6. Malcovati L, Karimi M, Papaemmanuil E, et al. SF3B1 mutation identifies a distinct subset of myelodysplastic syndrome with ring sideroblasts. *Blood*. 2015;126(2):233-241.

7. Papaemmanuil E, Cazzola M, Boultwood J, et al; Chronic Myeloid Disorders Working Group of the International Cancer Genome Consortium. Somatic SF3B1 mutation in myelodysplasia with ring sideroblasts. *N Engl J Med*. 2011;365(15):1384-1395.

8. Pimentel H, Parra M, Gee SL, Mohandas N, Pachter L, Conboy JG. A dynamic intron retention program enriched in RNA processing genes regulates gene expression during terminal erythropoiesis. *Nucleic Acids Res*. 2016;44(2):838-851.

9. Isono K, Mizutani-Koseki Y, Komori T, Schmidt-Zachmann MS, Koseki H. Mammalian polycomb-mediated repression of Hox genes requires the essential spliceosomal protein Sf3b1. *Genes Dev*. 2005;19(5):536-541.

10. De La Garza A, Cameron RC, Nik S, Payne SG, Bowman TV. Spliceosomal component Sf3b1 is essential for hematopoietic differentiation in zebrafish. *Exp Hematol*. 2016;44(9):826-837.e4.

11. Lawrence C. Advances in zebrafish husbandry and management. *Methods Cell Biol*. 2011;104:429-451.

12. Amsterdam A, Nissen RM, Sun Z, Swindell EC, Farrington S, Hopkins N. Identification of 315 genes essential for early zebrafish development. *Proc Natl Acad Sci USA*. 2004;101(35):12792-12797.

13. An M, Henion PD. The zebrafish sf3b1b460 mutant reveals differential requirements for the sf3b1 pre-mRNA processing gene during neural crest development. *Int J Dev Biol*. 2012;56(4):223-237.

14. Patnaik MM, Lasho TL, Hodnefield JM, et al. SF3B1 mutations are prevalent in myelodysplastic syndromes with ring sideroblasts but do not hold independent prognostic value. *Blood*. 2012;119(2):569-572.

15. Long Q, Meng A, Wang H, Jessen JR, Farrell MJ, Lin S. GATA-1 expression pattern can be recapitulated in living transgenic zebrafish using GFP reporter gene. *Development*. 1997;124(20):4105-4111.

16. Berghmans S, Murphey RD, Wienholds E, et al. tp53 mutant zebrafish develop malignant peripheral nerve sheath tumors. *Proc Natl Acad Sci USA*. 2005;102(2):407-412.

17. Brownlie A, Hersey C, Oates AC, et al. Characterization of embryonic globin genes of the zebrafish. *Dev Biol*. 2003;255(1):48-61.

18. Liao EC, Paw BH, Oates AC, Pratt SJ, Postlethwait JH, Zon LI. SCL/Tal-1 transcription factor acts downstream of cloche to specify hematopoietic and vascular progenitors in zebrafish. *Genes Dev*. 1998;12(5):621-626.

19. Detrich HW III, Kieran MW, Chan FY, et al. Intraembryonic hematopoietic cell migration during vertebrate development. *Proc Natl Acad Sci USA*. 1995;92(23):10713-10717.

20. Thisse C, Thisse B. High-resolution in situ hybridization to whole-mount zebrafish embryos. *Nat Protoc*. 2008;3(1):59-69.

21. Lieschke GJ, Oates AC, Crowhurst MO, Ward AC, Layton JE. Morphologic and functional characterization of granulocytes and macrophages in embryonic and adult zebrafish. *Blood*. 2001;98(10):3087-3096.

22. Love MI, Huber W, Anders S. Moderated estimation of fold change and dispersion for RNA-seq data with DESeq2. *Genome Biol*. 2014;15(12):550.

23. Robinson MD, McCarthy DJ, Smyth GK. edgeR: a Bioconductor package for differential expression analysis of digital gene expression data. *Bioinformatics*. 2010;26(1):139-140.

24. Shen S, Park JW, Lu ZX, et al. rMATS: robust and flexible detection of differential alternative splicing from replicate RNA-Seq data. *Proc Natl Acad Sci USA*. 2014;111(51):E5593-E5601.

25. Liberzon A, Birger C, Thorvaldsdóttir H, Ghandi M, Mesirov JP, Tamayo P. The Molecular Signatures Database (MSigDB) hallmark gene set collection. *Cell Syst*. 2015;1(6):417-425.

26. Subramanian A, Tamayo P, Mootha VK, et al. Gene set enrichment analysis: a knowledge-based approach for interpreting genome-wide expression profiles. *Proc Natl Acad Sci USA*. 2005;102(43):15545-15550.

27. Sun Z, Jin P, Tian T, Gu Y, Chen YG, Meng A. Activation and roles of ALK4/ALK7-mediated maternal TGFbeta signals in zebrafish embryo. *Biochem Biophys Res Commun*. 2006;345(2):694-703.

28. Danilova N, Kumagai A, Lin J. p53 upregulation is a frequent response to deficiency of cell-essential genes. *PLoS One*. 2010;5(12):e15938.

29. Kanehisa M, Furumichi M, Tanabe M, Sato Y, Morishima K. KEGG: new perspectives on genomes, pathways, diseases and drugs. *Nucleic Acids Res*. 2017;45(D1):D353-D361.

30. Kanehisa M, Sato Y, Kawashima M, Furumichi M, Tanabe M. KEGG as a reference resource for gene and protein annotation. *Nucleic Acids Res*. 2016; 44(D1):D457-D462.

31. Kanehisa M, Goto S. KEGG: Kyoto Encyclopedia of Genes and Genomes. *Nucleic Acids Res*. 2000;28(1):27-30.

32. Lefèvre C, Bondu S, Le Goff S, Kosmider O, Fontenay M. Dyserythropoiesis of myelodysplastic syndromes. *Curr Opin Hematol*. 2017;24(3):191-197.

33. Kim SJ, Letterio J. Transforming growth factor-beta signaling in normal and malignant hematopoiesis. *Leukemia*. 2003;17(9):1731-1737.

34. Kervestin S, Li C, Buckingham R, Jacobson A. Testing the faux-UTR model for NMD: analysis of Upf1p and Pab1p competition for binding to eRF3/Sup35p. *Biochimie*. 2012;94(7):1560-1571.

35. Lebrun JJ. The dual role of TGFβ in human cancer: from tumor suppression to cancer metastasis. *ISRN Mol Biol*. 2012;2012:381428.

36. Platzbecker U, Germing U, Götze KS, et al. Luspatercept for the treatment of anaemia in patients with lower-risk myelodysplastic syndromes (PACE-MDS): a multicentre, open-label phase 2 dose-finding study with long-term extension study. *Lancet Oncol*. 2017;18(10):1338-1347.

37. Suragani RN, Cadena SM, Cawley SM, et al. Transforming growth factor-β superfamily ligand trap ACE-536 corrects anemia by promoting late-stage erythropoiesis. *Nat Med*. 2014;20(4):408-414.

38. Zhou L, McMahon C, Bhagat T, et al. Reduced SMAD7 leads to overactivation of TGF-beta signaling in MDS that can be reversed by a specific inhibitor of TGF-beta receptor I kinase [published correction appears in *Cancer Res*. 2011;71(7):2806]. *Cancer Res*. 2011;71(3):955-963.

39. Chablais F, Jazwinska A. The regenerative capacity of the zebrafish heart is dependent on TGFβ signaling. *Development*. 2012;139(11):1921-1930.

40. Zermati Y, Fichelson S, Valensi F, et al. Transforming growth factor inhibits erythropoiesis by blocking proliferation and accelerating differentiation of erythroid progenitors. *Exp Hematol*. 2000;28(8):885-894.

41. Huang Y, Hale J, Wang Y, et al. SF3B1 deficiency impairs human erythropoiesis via activation of p53 pathway: implications for understanding of ineffective erythropoiesis in MDS. *J Hematol Oncol*. 2018;11(1):19.

42. Li AJ, Calvi LM. The microenvironment in myelodysplastic syndromes: Niche-mediated disease initiation and progression. *Exp Hematol*. 2017;55:3-18.

43. Mupo A, Seiler M, Sathiaseelan V, et al. Hemopoietic-specific Sf3b1-K700E knock-in mice display the splicing defect seen in human MDS but develop anemia without ring sideroblasts. *Leukemia*. 2017;31(3):720-727.

44. Obeng EA, Chappell RJ, Seiler M, et al. Physiologic expression of Sf3b1(K700E) causes impaired erythropoiesis, aberrant splicing, and sensitivity to therapeutic spliceosome modulation. *Cancer Cell*. 2016;30(3):404-417.

45. Darman RB, Seiler M, Agrawal AA, et al. Cancer-associated SF3B1 hotspot mutations induce cryptic 3′ splice site selection through use of a different branch point. *Cell Reports*. 2015;13(5):1033-1045.

46. Pellagatti A, Armstrong RN, Steeples V, et al. Impact of spliceosome mutations on RNA splicing in myelodysplasia: dysregulated genes/pathways and clinical associations. *Blood*. 2018;132(12):1225-1240.

47. Dolatshad H, Pellagatti A, Fernandez-Mercado M, et al. Disruption of SF3B1 results in deregulated expression and splicing of key genes and pathways in myelodysplastic syndrome hematopoietic stem and progenitor cells [published correction appears in Leukemia. 2015;29(8):1798]. *Leukemia*. 2015; 29(5):1092-1103.

48. Seiler M, Yoshimi A, Darman R, et al. H3B-8800, an orally available small-molecule splicing modulator, induces lethality in spliceosome-mutant cancers. *Nat Med*. 2018;24(4):497-504.

49. Eskens FA, Ramos FJ, Burger H, et al. Phase I pharmacokinetic and pharmacodynamic study of the first-in-class spliceosome inhibitor E7107 in patients with advanced solid tumors. *Clin Cancer Res*. 2013;19(22):6296-6304.